

Last Modified December 2, 2018

Large Misalignment between Stellar and Dust Bars in NGC 3488 Revealed by *Spitzer* and SDSS

Chen Cao^{1,2}, Hong Wu¹, Zhong Wang³, Luis C. Ho⁴, Jia-Sheng Huang³, Zu-Gan Deng^{5,1}

ABSTRACT

A large position angle misalignment between the stellar and dust bars in the late-type barred spiral NGC 3488 was discovered, using mid-infrared images from the *Spitzer Space Telescope* and optical images from the Sloan Digital Sky Survey (SDSS). The angle between the two distinctive bar patterns was measured to be $25^\circ \pm 2^\circ$, larger than most of the misalignments found previously in barred systems based on H α or H II/CO observations. The stellar bar is bright at optical and $3.6\mu\text{m}$, while the dust bar is more prominent in the $8\mu\text{m}$ band but also shows up in the SDSS u and g -band images, suggesting a rich interstellar medium environment harboring ongoing star formation. The angular misalignment between the two bars in NGC 3488 is unlikely to have been caused by spontaneous bar formation. We suggest that the two bars have different formation histories, and that the large misalignment was triggered by a tidal interaction with a small companion. A statistical analysis of a large sample of nearby galaxies with archival *Spitzer* data indicates that bar structure such as that seen in NGC 3488 is quite rare in the local Universe.

Subject headings: galaxies: individual(NGC 3488) — galaxies: spiral — galaxies: structure — infrared: galaxies

¹National Astronomical Observatories, Chinese Academy of Sciences, Beijing 100012, P. R. China; caochen@bao.ac.cn, hwu@bao.ac.cn

²Graduate School, Chinese Academy of Sciences, Beijing 100039, China

³Harvard-Smithsonian Center for Astrophysics, 60 Garden Street, Cambridge, MA 02138

⁴The Observatories of the Carnegie Institution of Washington, 813 Santa Barbara Street, Pasadena, CA 91101

⁵College of Physical Sciences, Graduate School, Chinese Academy of Sciences, P.O. Box 3908, 100039 Beijing, China

1. Introduction

Bar structure as a major non-axisymmetric feature on all scales is important in studying the morphology, mass and light distributions, star formation, gas dynamics and central activities of disk galaxies (Shlosman et al. 1990; Athanassoula 1992; Sellwood & Wilkinson 1993; Ho, Filippenko & Sargent 1997b). Theoretical models, including N-body and hydrodynamic simulations, generally confirm that bar formation is spontaneous and ubiquitous in disk evolution (Friedli & Benz 1993, 1995; Athanassoula & Bureau 1999; Debattista & Sellwood 2000). Because of the dissipative nature of the interstellar medium (ISM), gas motion in and around bar regions can be very different from the stellar orbits (Athanassoula 2000). This can consequently induce the formation of a separate “gas/dust bar”, which is of fundamental importance for understanding the ISM shocks and star formation in these galaxies (Athanassoula 1992).

Observationally, the gas/dust bar can often be seen as dust lanes, atomic and molecular gas concentrations, or isophotes of H II regions with active star formation (Martin & Friedli 1997; Crosthwaite, Turner & Ho 2000; Rautiainen et al. 2005; Hernandez et al. 2005). As predicted by theoretical models (Friedli & Benz 1993, 1995), there is a small position angle misalignment between the gas/dust and stellar bars, usually of a few (and up to 10) degrees, in the sense that the former is *leading* when the disk’s pattern rotation is taken into consideration. Kenney, Scoville & Wilson (1991) found the gaseous bar is offset from the major axis of the stellar distribution by $24^\circ \pm 6^\circ$ in M 101. Crosthwaite, Turner & Ho (2000) found that the central gas bar as indicated by H I map leads the stellar bar by almost 10° in the late-type galaxy IC 342. Similarly, Rozas, Zurita & Beckman (2000) identified a large sample of H II regions in barred galaxy NGC 3359 and showed a position angle misalignment of a few degrees exists in H α and I-band images. They also pointed out that the *u*-band image of this galaxy shows a bar pattern more aligned with H α , further suggesting massive star formation “at the leading edge of the bar”. Sheth et al. (2002) found two of the six spirals from the BIMA Survey of Nearby Galaxies have large angle misalignments between stellar and gas (CO) bars. Understanding the misalignment between stellar and gas/dust bars and their formation scenarios is crucial for studying the ISM properties and star formation processes taking place in environments where gas dynamics are strongly perturbed (Martin & Friedli 1997), and also offers a good opportunity to study dynamical properties and secular evolution of barred galaxies (Kormendy & Kennicutt 2004).

Nevertheless, determination of gas bars based on H I maps, because of their rather low spatial resolution, can only be done in a few of the nearest giant galaxies, while optical data such as H α images suffer from uncertainties associated with heavy dust extinction. The *Spitzer Space Telescope*’s (Werner et al. 2004) observations in the mid-infrared, with

its higher sensitivity and better angular resolution than previous observations (e.g., *ISO*), provide a new opportunity to study both stellar and gas/dust structures in galaxies (e.g., Pahre et al 2004; Wang et al. 2004). In particular, the four Infrared Array Camera (IRAC; Fazio et al. 2004) bands from 3.6 to 8.0 μm probe both stellar continuum and warm dust emissions (of the so-called polycyclic aromatic hydrocarbon, or PAH, and dust continuum emissions) with identical spatial sampling, thus enabling a powerful probe to compare non-axisymmetric features such as bar structures involving gas/dust and stellar mass. Recently, *Spitzer* observations of nearby galaxies have demonstrated the importance of using mid-infrared images for studying galaxy secular evolution driven by bar instabilities (e.g., Fisher 2006; Regan et al. 2006).

In this paper, we present an analysis of data from *Spitzer* and SDSS of the late-type barred spiral galaxy NGC 3488. Previous studies show that, with an estimated distance of 39.9 Mpc (at this distance, 1" corresponds to \sim 193 parsecs) and a total infrared luminosity of $L_{\text{TIR}} \approx 4.6 \times 10^9 L_{\odot}$ (Bell 2003), NGC 3488 [Hubble type SB(s)c] has a weak bar (\sim 1.5 kpc), with spiral arms beginning at the bar's end but without an inner ring. This is consistent with the conventional view that bars in most late-type spirals are relatively weak (Erwin 2005), and that weak bars tend to produce a SB(s) type response (Kormendy & Kennicutt 2004). The data reduction is presented in §2, and results on the bar structures in NGC 3488 with multi-wavelengths analysis are described in §3. Possible explanations of the large misalignment between the two bars are discussed in §4.

2. Data Reduction

Broad-band infrared images of NGC 3488 were acquired with IRAC on board *Spitzer*. The Basic Calibrated Data (BCD) were part of the Lockman Hole field in the *Spitzer* Wide-field Infrared Extragalactic (SWIRE) Survey (Lonsdale et al. 2003). Following the preliminary data reduction by the *Spitzer* Science Center pipeline, images of each of the four IRAC bands (3.6, 4.5, 5.8 and 8 μm) were mosaicked, after pointing refinement, distortion correction and cosmic-ray removal (Fazio et al. 2004; Huang et al. 2004; Wu et al. 2005; Surace et al. 2005). The mosaicked images have pixel sizes of 0.6" and angular resolutions (full width at half maximum, FWHM) of 1.9", 2.0", 1.9" and 2.2" for the four bands, respectively. The angular resolution of IRAC 8 μm images (\sim 2.2") is significantly improved over that of pre-*Spitzer* data at similar wavelengths (e.g., \sim 10" for ISOCAM LW2 at 7 μm ; Roussell et al. 2001).

In order to derive the dust-only 8 μm component (PAH and dust continuum emissions), we remove the stellar continuum from the IRAC 8 μm image by subtracting a scaled IRAC

$3.6\mu\text{m}$ image (assuming that the $3.6\mu\text{m}$ emission is entirely due to old stellar population):

$$f_\nu(8\mu\text{m})_{\text{dust}} = f_\nu(8\mu\text{m}) - \eta_{8\mu\text{m}} f_\nu(3.6\mu\text{m}),$$

where the scaling factor $\eta_{8\mu\text{m}} = 0.232$ was calculated based on *Starburst99* synthesis model (Leitherer et al. 1999), assuming solar metallicity and a Salpeter initial mass function between 0.1 and $120 M_\odot$. This approach has been adopted in several previous works (e.g., Helou et al. 2004; Dale et al. 2005; Wu et al. 2005; Regan et al. 2006; Bendo et al. 2006) for studying dust emissions and the $7.7\mu\text{m}$ PAH feature based on broad-band measurements, and shown to be effective.

The five-band optical images (u, g, r, i, z) and the fiber spectrum for the central region ($3''$ diameter) of NGC 3488 were taken from the SDSS data archive (York et al. 2000; Stoughton et al. 2002). The background in each band was subtracted by fitting a low-order Legendre polynomial to it, after masking out all bright sources (Zheng et al. 1999; Wu et al. 2002).

3. Results

3.1. Multi-wavelength View of Bar Structures in NGC 3488

The four-band IRAC images of NGC 3488 are shown in Figure 1. We find that NGC 3488 has two bars that are bright in either stellar emission (at 3.6 and $4.5\mu\text{m}$) or warm dust emission (at $8\mu\text{m}$). We took the conventional approach of treating the bar as an elliptical feature for measuring its semi-major axis a and position angle PA. They can be measured with a fitting routine such as the `ellipse` task in IRAF. The PAs are approximately 36° , 36° , 20° , 15° for the bars in the 3.6 , 4.5 , 5.8 , $8\mu\text{m}$ band, respectively. Uncertainties of the position angles are estimated to be $\pm 2^\circ$, derived from the deviation of PAs along the major axis of the bar. Taking the mean of the two shorter wavelength bands as representing the stellar bar, we measured that it trails the “dust bar,” traced primarily by the continuum-subtracted $8\mu\text{m}$ emission (Fig. 2c), by a large position angle difference. Spiral arms with bright knots are also visible in the $8\mu\text{m}$ image: they appear to begin at the end of the dust bar (Fig. 2d).

For the SDSS images, the PA of the bar was also measured using `ellipse`. The PA of the optical bar measured in this way is nearly identical ($\sim 40^\circ$) in the SDSS g , r , i , z -band images, and is also spatially coincident, within the measurement uncertainty of $\sim \pm 2^\circ$, with that of the IRAC 3.6 and $4.5\mu\text{m}$ images, but trails the dust bar at $8\mu\text{m}$ by 25° (Fig. 2b). However, the bar in the SDSS u -band is quite different from that in the other SDSS bands:

at PA $\approx 15^\circ$, it is instead much better aligned with the dust bar bright at IRAC 8 μm (Fig. 2a).

The deprojected values of the relative length [$L_b(i)$] and the misalignment between the stellar and dust bars [$\theta(i)$] are calculated using the equations given by Martin (1995):

$$L_b(i) = \frac{2a[\cos^2(\phi_a) + \sec^2(i)\sin^2(\phi_a)]^{1/2}}{D_{25}}$$

$$\theta(i) = \arctan[\cos(i)\tan(\phi_{a;8\mu\text{m}})] - \arctan[\cos(i)\tan(\phi_{a;\text{stellar}})],$$

where i is the inclination angle of NGC 3488 ($\sim 49.5^\circ$, calculated using the formula given by Bottinelli et al. 1983), a is the length of the semi-major axis, ϕ_a is the angle between the bar (dust or stellar) and the node lines (the major axis defines the PA of the galaxy, $\sim 175^\circ$), and D_{25} is the diameter of NGC 3488 at a B -band surface brightness of 25 mag arcsec $^{-2}$ (~ 1.86 arcmin).¹ These parameters of the bars are summarized in Table 1. The angular misalignment between the optical and infrared dust bars, $\theta(i)$, is approximately 20° after correcting for inclination effect. Uncertainties of these parameters can be as large as 20%, due mostly to simplistic assumptions concerning projection effects and the difficulty in decoupling the bar from the bulge (Martin 1995; Martin & Friedli 1997), especially in the IRAC 8 μm image. Nevertheless, this angular misalignment, assuming it represents the misalignment between the dust and stellar bars, belongs to one of the largest misalignments found in previous observations or in typical numerical simulations.

Besides the two bright bars, a faint and clumpy bar-like structure appears to be present in the SDSS g -band image (Fig. 3a). We use two different techniques to enhance the visibility of this structure: unsharp masking (e.g., Walterbos, Braun, & Kennicutt 1994; Fig. 3b) and deconvolution (Fig. 3c). Unsharp masking was made by using a 2-pixel wide (2σ) Gaussian filter. The deconvolution was performed with the task `lucy` (Lucy 1974) in IRAF, using a point-spread function derived from the associated `psField` file of the SDSS data; the total number of iterations is 30. The PA of this faint bar-like structure is approximately $15^\circ \pm 2^\circ$, so it is spatially coincident with the bars in u -band and 8 μm images.

3.2. Stellar Populations in Bars

The bars bright at optical (SDSS) and IRAC 3.6, 4.5 μm are known to be dominated by old stellar population. Gadotti & de Souza (2006) showed that the bar color index

¹The PA, D_{25} , and R_{25} of NGC 3488 were taken from The Third Reference Catalogue of Bright Galaxies (de Vaucouleurs et al. 1991).

can be used as an indicator of the bar age: old bars are on average redder than young ones. The SDSS $g - r$ and $g - i$ colors of the stellar bar of NGC 3488 were compared with an instantaneous burst model calculated based on GALAXEV (Bruzual & Charlot 2003), adopting a Salpeter initial mass function and solar metallicity as initial conditions. This comparison shows that the stellar bar bright in optical and IRAC 3.6 and $4.5\mu\text{m}$ bands is evolved, with a mean age of the order of 4 Gyr.

The bar bright at $8\mu\text{m}$ is dominated by the strong $7.7\mu\text{m}$ PAH feature and warm dust continuum emission from very small grains, while the bar shown in the IRAC $5.8\mu\text{m}$ image is probably a mixture of stellar and dust ($6.2\mu\text{m}$ PAH and warm dust) components. From the correlation between $8\mu\text{m}$ dust emission and star formation activities (Wu et al. 2005; Calzetti et al. 2005) and the previous result that $8\mu\text{m}$ dust and $24\mu\text{m}$ hot dust emission are well correlated on kiloparsec scales² (e.g., Bendo et al. 2006), we suggest that the dust bar seen at $8\mu\text{m}$ is associated with young stars and thus represents recent star forming activity. Some authors (e.g., Regan et al. 2006; R. C. Kennicutt, priv. comm.), however, argue that PAH emission is likely a better tracer of the general ISM rather than star-forming regions heated by young, massive stars. The coincidence of the bar shown in the u -band with the bar bright at $8\mu\text{m}$ (Fig. 2a) confirms that there exists a young stellar population in the dust bar region.

3.3. Star Formation Rates

The star formation rate (SFR) in the bar region of NGC 3488 can be estimated using either the $\text{H}\alpha$ line flux or the $8\mu\text{m}$ dust emission. The SDSS spectrum, taken through a $3''$ -diameter (~ 0.58 kpc) fiber, indicates that the central region can be classified as an “H II nucleus” (Ho, Filippenko & Sargent 1997a), one whose main source of ionizing photons derives from young stars. The $\text{H}\alpha$ -based SFR is calculated using Equation B3 of Hopkins et al. (2003), after correcting for extinction using the observed Balmer decrement (Calzetti 2001):

$$SFR_{\text{H}\alpha}(M_{\odot}\text{yr}^{-1}) = 4\pi D_{\text{l}}^2 S_{\text{H}\alpha} \left(\frac{S_{\text{H}\alpha}/S_{\text{H}\beta}}{2.86} \right)^{2.114} \frac{1}{1.27 \times 10^{34}},$$

where $S_{\text{H}\alpha}$ and $S_{\text{H}\beta}$ are the stellar absorption-corrected line fluxes, derived from the emission-line catalog given by MPA-SDSS (Tremonti et al. 2004). The measured SFR for the central $3''$ based on $\text{H}\alpha$ is $0.0077 M_{\odot} \text{ yr}^{-1}$.

²MIPS $24\mu\text{m}$ emission, which is mainly due to hot dust emission from very small grains, is thought to be a good measure of the SFR in galaxies (e.g., Wu et al. 2005; Calzetti et al. 2005; Perez-Gonzalez et al. 2006).

To estimate the SFR along the bar, we use the $8\mu\text{m}$ dust emission, which is thought to be a good measure of the SFR in galaxies (Wu et al. 2005). From Equation 4 of Wu et al. (2005):

$$SFR_{8\mu\text{m dust}}(M_{\odot}\text{yr}^{-1}) = \frac{\nu L_{\nu}(8\mu\text{m dust})}{1.57 \times 10^9 L_{\odot}}.$$

An aperture of $3''$ diameter was selected for measuring the SFR centered on the nucleus using the dust-only $8\mu\text{m}$ image, to enable a sensible comparison with the SFR derived from the $\text{H}\alpha$ flux. The SFR measured in this way is $0.0079 M_{\odot} \text{ yr}^{-1}$, consistent with that derived from $\text{H}\alpha$. This result indicates that the $8\mu\text{m}$ dust emission can be used as a reliable tracer of the SFR in the central region of galaxies, at least for the case of NGC 3488. The enhanced $8\mu\text{m}$ emission in the central region of NGC 3488 is consistent with the result that barred galaxies tend to have strong central excesses in $8\mu\text{m}$ emission (Regan et al. 2006), which suggests that bars induce gas inflows toward the center of galaxies as an internal process of galaxy secular evolution (Kormendy & Kennicutt 2004). We also estimated the total SFR along the bar after excluding the contribution from the central region. The photometry was performed on the dust-only $8\mu\text{m}$ image using an ellipse with a semi-major axis of $3''$ and an ellipticity of 0.5, chosen to match the isocontour of the bar. The measured SFR for the bar and nucleus is $\sim 0.0150 M_{\odot} \text{ yr}^{-1}$, which implies that the SFR along the bar is roughly $0.0072 M_{\odot} \text{ yr}^{-1}$, comparable to the value at the nucleus.

4. Discussion

4.1. Possible Formation Scenarios of the Misalignment Between Bars in NGC 3488

Martin & Friedli (1997) found that the $\text{H}\alpha$ bars (tracing young stars and H II regions) and stellar bars are misaligned by up to 10° among 11 barred galaxies. Friedli & Benz (1993, 1995), using their N-body + SPH simulations of spontaneous bar formation, showed that the H II regions tend to lead the stellar bar by an angle of several degrees. In these simulations the misalignments between bars are similar to those observed, and they occur as a result of orbit crossings of gas motion, mostly at early epochs during the formation of a strong, fast-rotating bar in the absence of an inner Lindblad resonance (Martin & Friedli 1997). The best example is NGC 3359, in which star formation is completely absent in the galaxy nucleus (Martin & Friedli 1997), and the age of the bar is young (~ 400 Myr; Martin & Roy 1995). But this is unlikely to be the case in NGC 3488, due to the fact that the age of its stellar bar (~ 4 Gyr) is much older than bars in the spontaneous bar formation scenario (e.g., NGC 3359).

Alternatively, perhaps the morphology of this galaxy represents an episode shortly after the capture of a small, secondary galaxy. In such a galaxy merger scenario, the stellar and dust bars may have different formation histories. The stellar bar may have formed previously as in a spontaneous formation scenario, and the dust bar could be tidally induced later from a dwarf galaxy swallowed by NGC 3488. The different stellar populations in the stellar and dust bars (see §3.2) also support this scenario. Berentzen et al. (2003) investigated the dynamical effects of the interaction between an initially barred galaxy and a small companion, using N-body/SPH numerical simulations. They found that the interactions can produce offset bars, nuclear and circumnuclear disks, and tidal arms connected to the end of the bar. Based on their results that the fate of the stellar bar is determined by the impact position, we speculate that in NGC 3488 there may have been an impact on the bar major axis when the bar was weak. In such a case, the tidal force exerted on the bar does not disrupt much the bar structure (i.e., the stellar bar survived after the impact). The nearby bright, compact object toward the northeast of the SDSS images (see Fig. 2b), identified as SDSS J110124.04+574045.1, is a plausible candidate for a dwarf galaxy that may have hit NGC 3488. Its colors are very blue ($u - g = 0.309$, $g - r = -0.222$, $r - i = -0.757$) and similar to those of irregular galaxies (Fukugita et al. 1995). And its absolute magnitude (-12.73 , -13.59 , -13.93 , -13.82 , -13.81 for u , g , r , i , z , respectively) are located at the faint end of the luminosity function of extremely low-luminosity galaxies (Blanton et al. 2005), if we assume that its distance is the same as that of NGC 3488 (39.9 Mpc). However, we cannot exclude the possibility that it is a foreground white dwarf star superposed on NGC 3488, since its very blue colors are consistent with those of spectroscopically identified white dwarf stars in SDSS (Kleinman et al. 2004).

4.2. Bar Pattern Speed and the Misalignment Between Bars

The misalignment between dust and stellar bars may also be related to the pattern speed of the bar (Elmegreen et al. 1996). Increasing misalignment was found with decreasing pattern speed in several early hydrodynamic simulations (Sanders & Tubbs 1980; Combes & Gérin 1985). Miwa & Noguchi (1998), from their 3D N-body simulations on tidal encounters between disk and perturbing galaxies, found that tidally induced bars sometimes rotate quite slowly. In the late-impact models of Berentzen et al. (2003), they found that the bar pattern speed decreases temporarily by 30% shortly after the impact. Berentzen et al. (2004), using numerical simulations of either stellar or stellar plus gas disks, also found that stellar bars formed and regenerated by tidal interactions always have lower pattern speeds than those formed spontaneously in the corresponding isolated models. NGC 289, a late-type barred spiral (type SABbc), may have a similarly large misalignment between its stellar bar (traced

by K -band image of 2MASS; Jarrett et al. 2003) and dust bar (*ISO* 7 μm ISOCAM LW2 image; Roussel et al. 2001), and it is known to have a very slow bar pattern speed. Rautiainen et al. (2005) report that NGC 289 has $R_{\text{CR}}/R_{\text{bar}} \approx 2.63$, where $R_{\text{CR}}/R_{\text{bar}}$ is the ratio of the corotation resonance radius to the bar radius, and is often used to indicate the pattern speed of a stellar bar. A bar is fast if $R_{\text{CR}}/R_{\text{bar}} \leq 1.4$; otherwise it is slow (Debattista & Sellwood 2000). Therefore, the large misalignment between bars in NGC 3488 could presumably be related to a slow bar pattern speed as well. The bar’s rotation may be slowed down by angular momentum transfer and dynamical friction between the bar and a dark halo in the inner parts of the galaxy (Sellwood & Wilkinson 1993; Tremaine & Ostriker 1999; Pérez et al. 2004; Sellwood 2006; Sellwood & Debattista 2006).

4.3. Frequency of Large Misalignments Between Bars Among Galaxies Revealed By *Spitzer*

Large misalignments ($>10^\circ$) between stellar bars (bright at optical and 3.6 μm) and dust bars (shown at 8 μm) are quite rare among nearby barred galaxies with archival *Spitzer* data. We have examined ~ 50 barred spirals (SB and SAB) in the *Spitzer* Infrared Nearby Galaxies Survey (SINGS, Kennicutt et al. 2003) and in the Mid-IR Hubble Atlas of Galaxies (a *Spitzer* GTO program, PID: #69, PI: G. Fazio; see also Pahre et al. 2004), and found that *none* of them shows a bar misalignment as large as that found in NGC 3488. Most of the galaxies only have a single old stellar bar, which is bright at IRAC 3.6 and 4.5 μm but absent at 8 μm (e.g., NGC 7080). Others that have younger bars always show good alignment between 3.6 and 8 μm (e.g., NGC 7479, consistent with the previous result that no misalignment was observed between its H α and stellar bars; Martin & Friedli 1997). This statistical evidence indicates that the bar structure seen in NGC 3488 is quite rare among barred galaxies in the local Universe, and that the misalignment between bars may be a short-lived phenomenon in the evolutionary history of the galaxy. However, any firm conclusion must await a quantitative analysis of a large, well-defined, and unbiased sample of barred galaxies. The case study of NGC 3488 presented lays the foundation for such a systematic study.

5. Summary

Using mid-infrared images from *Spitzer* and optical images from SDSS, we show that the late-type barred spiral galaxy NGC 3488 contains two misaligned bars, one composed of old stars and the other young stars and dust. The angle between the two bar patterns

($\sim 25^\circ$) is among the largest ever reported. The stellar bar is bright in the optical and in the IRAC 3.6 and $4.5\mu\text{m}$ bands, and is dominated by old stars. The dust bar is more prominent in the $8\mu\text{m}$ band, but also shows up in the SDSS u and g bands; it traces regions of recent or ongoing star formation. The dust bar could be tidally induced by a dwarf galaxy swallowed by NGC 3488, and the large bar misalignment may be related to a relatively slow bar pattern speed in NGC 3488. From examination of mid-infrared images of a large sample of nearby barred galaxies with archival *Spitzer* data, we find that bar structure such as that found in NGC 3488 is quite rare in the local Universe.

To further test the hypothesis that the large bar misalignment in NGC 3488 was triggered by a recent merger, it would be desirable to obtain deeper imaging observations of the system in order to search for morphological features suggestive of tidal interactions. Obtaining a spectrum of the candidate dwarf galaxy would help validate its physical association with NGC 3488. Additional numerical simulations will help to validate whether two large-scale bars can coexist over long time scales, since it is possible that the competing torques will introduce chaos to the system (I. Berentzen, priv. comm.).

We thank X.-Y. Xia, S. Mao, Y. Gao, R. Kennicutt, I. Berentzen, G. Bendo, R.-Q. Mao, J.-Y. Wei, J.-L. Wang for advice and helpful discussions, and C.-N. Hao, F.-S. Liu for their capable assistance throughout the process of *Spitzer* data reductions. This project is supported by NSFC No.10273012, No.10333060, No.10473013, No.10373008. This work is based in part on observations made with the *Spitzer Space Telescope*, which is operated by the Jet Propulsion Laboratory, California Institute of Technology under NASA contract 1407. Funding for the SDSS and SDSS-II has been provided by the Alfred P. Sloan Foundation, the Participating Institutions, the National Science Foundation, the U.S. Department of Energy, the National Aeronautics and Space Administration, the Japanese Monbukagakusho, the Max Planck Society, and the Higher Education Funding Council for England. The SDSS Web Site is <http://www.sdss.org/>. The SDSS is managed by the Astrophysical Research Consortium for the Participating Institutions. The Participating Institutions are the American Museum of Natural History, Astrophysical Institute Potsdam, University of Basel, Cambridge University, Case Western Reserve University, University of Chicago, Drexel University, Fermilab, the Institute for Advanced Study, the Japan Participation Group, Johns Hopkins University, the Joint Institute for Nuclear Astrophysics, the Kavli Institute for Particle Astrophysics and Cosmology, the Korean Scientist Group, the Chinese Academy of Sciences (LAMOST), Los Alamos National Laboratory, the Max-Planck-Institute for Astronomy (MPIA), the Max-Planck-Institute for Astrophysics (MPA), New Mexico State University, Ohio State University, University of Pittsburgh, University of Portsmouth, Princeton University, the United States Naval Observatory, and the University of Washington.

Facilities: Spitzer, Sloan.

REFERENCES

Athanassoula, E. 1992, MNRAS, 259, 328

Athanassoula, E., & Bureau, M. 1999, ApJ, 522, 699

Athanassoula, E. 2000, ASP Conf. Ser. 221, Stars, Gas and Dust in Galaxies: Exploring the Links, ed. D. Alloin, K. Olsen, & G. Galaz (San Francisco: ASP), 243

Bell, E. F. 2003, ApJ, 586, 794

Bendo, G. J., et al. 2006, ApJ, in press (astro-ph/0607669)

Berentzen, I., Athanassoula, E., Heller, C. H., & Fricke, K. J. 2003, MNRAS, 341, 343

Berentzen, I., Athanassoula, E., Heller, C. H., & Fricke, K. J. 2004, MNRAS, 347, 220

Blanton, M. R., Lupton, R. H., Schlegel, D. J., Strauss, M. A., Brinkmann, J., Fukugita, M., & Loveday, J. 2005, ApJ, 631, 208

Bottinelli, L., Gouguenheim, L., Paturel, G., & de Vaucouleurs, G. 1983, A&A, 118, 4

Bruzual, G., & Charlot, S. 2003, MNRAS, 344, 1000

Calzetti, D. 2001, PASP, 113, 1449

Calzetti, D., et al. 2005, ApJ, 633, 871

Combes, F., & Gerin, M. 1985, A&A, 150, 327

Crosthwaite, L. P., Turner, J. L., & Ho, P. T. P. 2000, AJ, 119, 1720

Dale, D. A., et al. 2005, ApJ, 633, 857

Debattista, V. P., & Sellwood, J. A. 2000, ApJ, 543, 704

de Vaucouleurs, G., de Vaucouleurs, A., Corwin, H. G., Buta, R. J., Paturel, G. & Fouque, P. 1991, Third Reference Catalogue of Bright Galaxies (New York: Springer)

Elmegreen, B. G., Elmegreen, D. M., Chromey, F. R., Hasselbacher, D. A., & Bissell, B. A. 1996, AJ, 111, 2233

Erwin, P. 2005, MNRAS, 364, 283

Fazio, G. G., et al. 2004, ApJS, 154, 10

Fisher, D. B. 2006, ApJ, 642, L17

Friedli, D., & Benz, W. 1993, A&A, 268, 65

Friedli, D., & Benz, W. 1995, A&A, 301, 649

Fukugita, M., Shimasaku, K., & Ichikawa, T. 1995, PASP, 107, 945

Gadotti, D. A., & de Souza, R. E. 2006, ApJS, 163, 270

Helou, G., et al. 2004, ApJS, 154, 253

Hernandez, O., Wozniak, H., Carignan, C., Amram, P., Chemin, L., & Daigle, O. 2005, ApJ, 632, 253

Ho, L. C., Filippenko, A. V., & Sargent, W. L. W. 1997a, ApJ, 487, 579

Ho, L. C., Filippenko, A. V., & Sargent, W. L. W. 1997b, ApJ, 487, 591

Hopkins, A. M., et al. 2003, ApJ, 599, 971

Huang, J.-S., et al. 2004, ApJS, 154, 44

Jarrett, T. H., Chester, T., Cutri, R., Schneider, S. E., & Huchra, J. P. 2003, AJ, 125, 525

Kenney, J. D. P., Scoville, N. Z., & Wilson, C. D. 1991, ApJ, 366, 432

Kennicutt, R. C., et al. 2003, PASP, 115, 928

Kleinman, S. J., et al. 2004, ApJ, 607, 426

Kormendy, J., & Kennicutt, R. C. 2004, ARA&A, 42, 603

Leitherer, C., et al. 1999, ApJS, 123, 3

Lonsdale, C. J., et al. 2003, PASP, 115, 897

Lucy, L. B. 1974, AJ, 79, 745

Martin, P. 1995, AJ, 109, 2428

Martin, P., & Friedli, D. 1997, A&A, 326, 449

Martin, P., & Roy, J.-R. 1995, *ApJ*, 445, 161

Miwa, T., & Noguchi, M. 1998, *ApJ*, 499, 149

Pahre, M. A., Ashby, M. L. N., Fazio, G. G., & Willner, S. P. 2004, *ApJS*, 154, 235

Pérez, I., Fux, R., & Freeman, K. 2004, *A&A*, 424, 799

Perez-Gonzalez, P. G., et al. 2006, *ApJ*, in press (astro-ph/0605605)

Rautiainen, P., Salo, H., & Laurikainen, E. 2005, *ApJ*, 631, L129

Regan, M. W., et al. 2006, *ApJ*, preprint doi:10.1086/505382'

Roussel, H., et al. 2001, *A&A*, 369, 473

Rozas, M., Zurita, A., & Beckman, J. E. 2000, *A&A*, 354, 823

Sanders, R. H., & Tubbs, A. D. 1980, *ApJ*, 235, 803

Sellwood, J. A., & Wilkinson, A. 1993, *Reports of Progress in Physics*, 56, 173

Sellwood, J. A. 2006, *ApJ*, 637, 567

Sellwood, J. A., & Debattista, V. P. 2006, *ApJ*, 639, 868

Sheth, K., Vogel, S. N., Regan, M. W., Teuben, P. J., Harris, A. I., & Thornley, M. D. 2002, *AJ*, 124, 2581

Shlosman, I., Begelman, M. C., & Frank, J. 1990, *Nature*, 345, 679

Stoughton, C., et al. 2002, *AJ*, 123, 485

Surace, J. A., et al. 2005, 'The SWIRE Data Release 2: Image Atlases and Source Catalogs for ELAIS-N1, ELAIS-N2, XMM-LSS, and the Lockman Hole'

Tremaine, S., & Ostriker, J. P. 1999, *MNRAS*, 306, 662

Walterbos, R. A. M., Braun, R., & Kennicutt, R. C., Jr. 1994, *AJ*, 107, 184

Wang, Z., et al. 2004, *ApJS*, 154, 193

Werner, M. W., et al. 2004, *ApJS*, 154, 1

Wu, H., et al. 2002, *AJ*, 123, 1364

Wu, H., Cao, C., Hao, C.-N., Liu, F.-S., Wang, J.-L., Xia, X.-Y., Deng, Z.-G., & Young, C. K.-S. 2005, ApJ, 632, L79

York, D. G., et al. 2000, AJ, 120, 1579

Zheng, Z., et al. 1999, AJ, 117, 2757

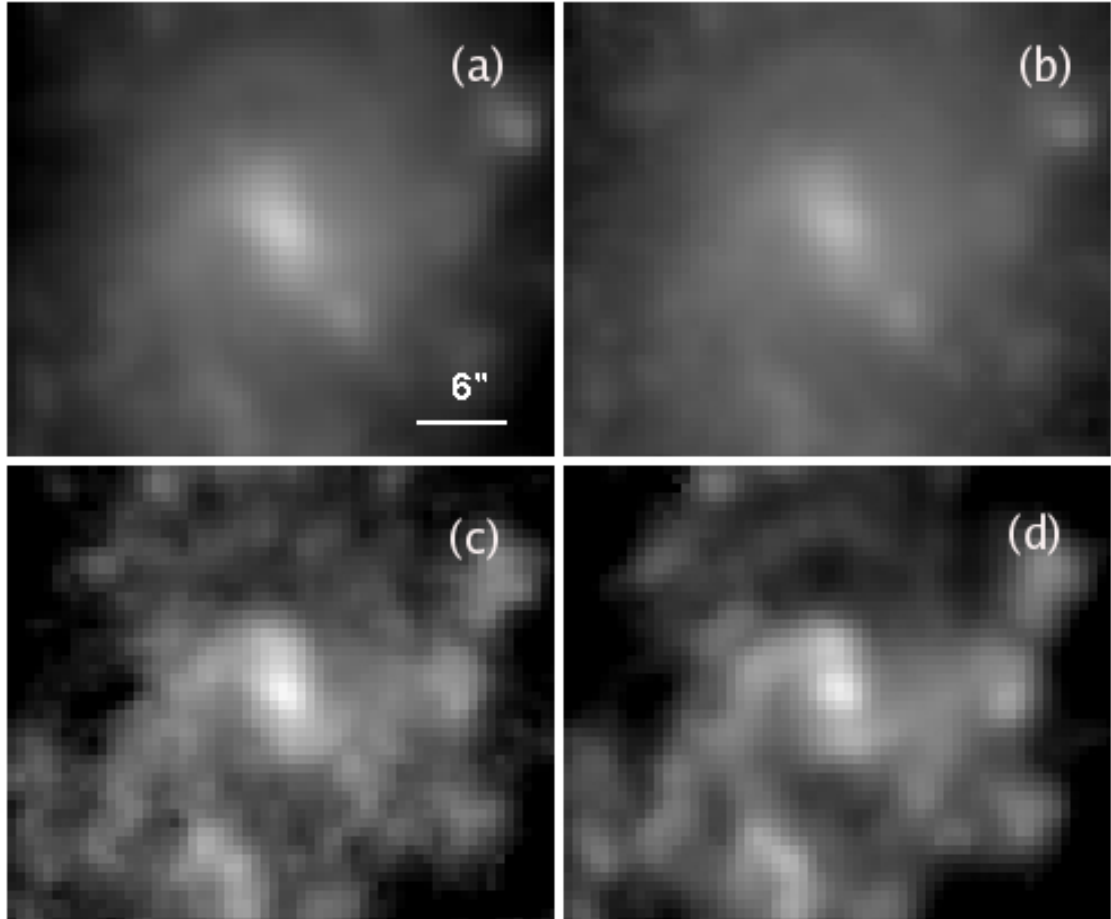


Fig. 1.— The *Spitzer* IRAC four-band images [from (a) to (d): 3.6, 4.5, 5.8, 8 μ m] of the bar region in NGC 3488. North is up; East is to the left. The stellar bar bright at 3.6 and 4.5 μ m and the dust bar bright at 8 μ m are misaligned by a large angle.

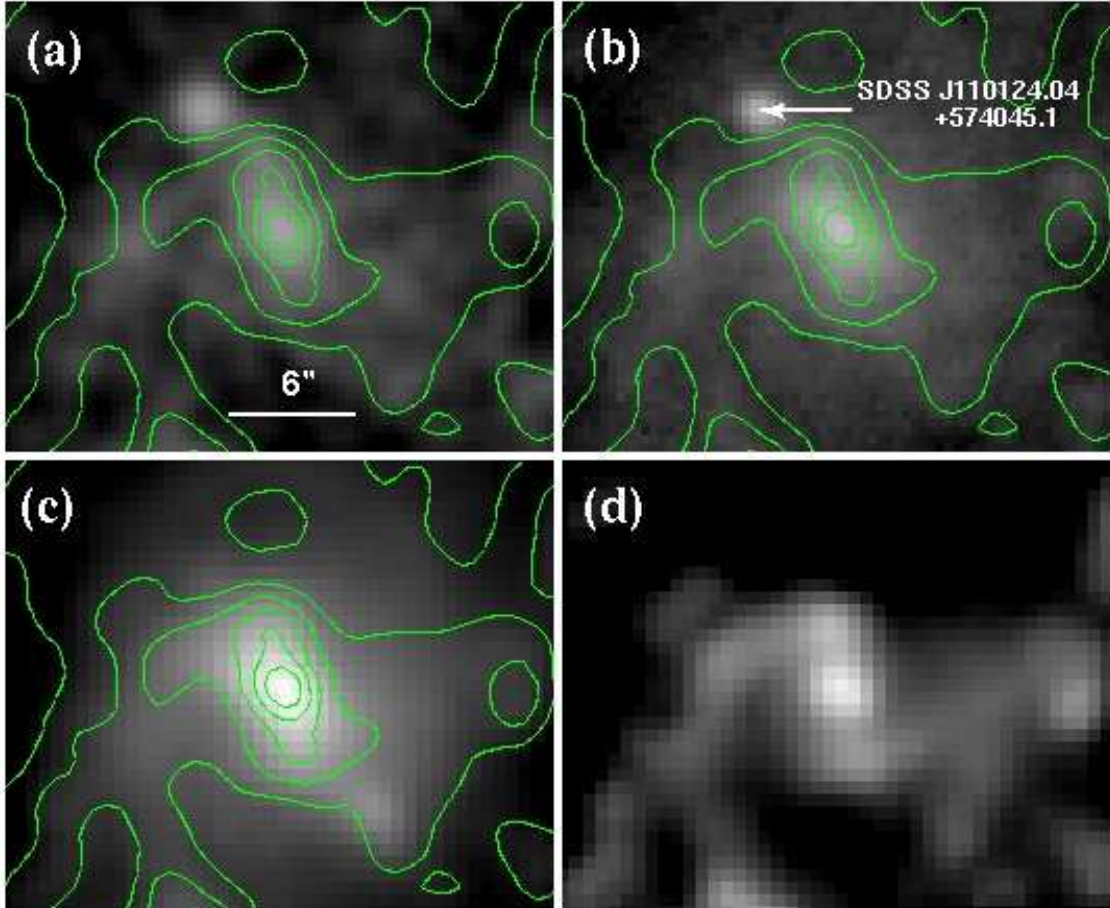


Fig. 2.— From (a) to (d): the SDSS *u*-band, *g*-band, IRAC $3.6\mu\text{m}$, and dust-only $8\mu\text{m}$ images of the bar region in NGC 3488. North is up; East is to the left. The *u*-band image was smoothed using a 2-pixel wide (2σ) Gaussian filter. Contours of the dust-only $8\mu\text{m}$ image are superposed on the *u*-band, *g*-band, and IRAC $3.6\mu\text{m}$ images. A large misalignment by an apparent angle (θ) of about 25° is shown between the two bright bars at optical and mid-infrared. A nearby compact, bright object (SDSS J110124.04+574045.1) is shown in the northeast of the SDSS images.

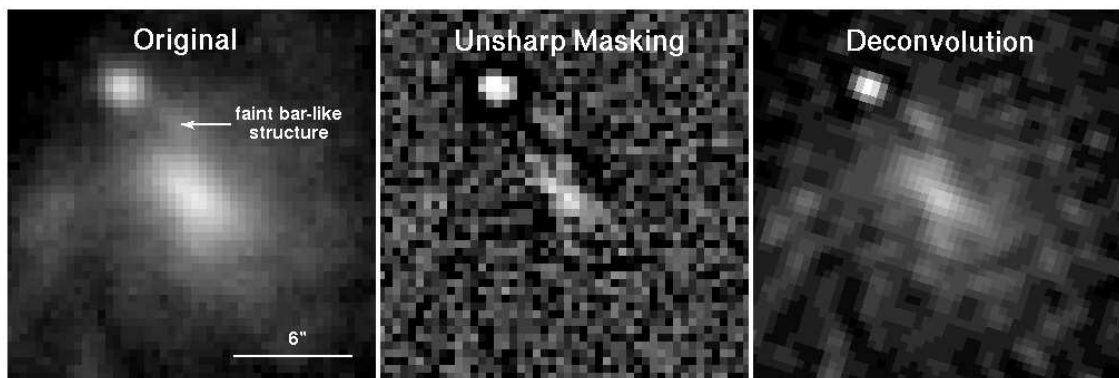


Fig. 3.— The original (left), unsharp-masked (middle), and deconvolved (right) SDSS g -band images of the bar region in NGC 3488. North is up; East is to the left. A faint and clumpy bar-like structure is suggested in the unsharp-masked and deconvolved images.

Table 1. Bar Properties

Bars	$a["]$ (a)	$L_b(i)$ (b)	PA[$^{\circ}$] (c)	$\theta[{}^{\circ}]$ (d)	$\theta(i)[{}^{\circ}]$ (e)	Image (f)
Stellar Bar	4.2	0.111	40.0	25.0	19.7	SDSS g band
Dust Bar	3.0	0.067	15.0			IRAC $8\mu\text{m}$

Notes.—(a) The length of semi-major axis of the bar. (b) The relative length of the bar. (c) Position angle measured in the conventional manner, from North through East. (d) The measured angular misalignment between stellar and dust bars. (e) The angular misalignment after correcting for inclination effect. (f) Image used for bar measurement.